

## HYDROMAGNETIC $\alpha\Omega$ -TYPE DYNAMOS WITH FEEDBACK FROM LARGE SCALE MOTIONS

A. BRANDENBURG<sup>1,2</sup>, D. MOSS<sup>3</sup>, G. RÜDIGER<sup>4</sup> AND I. TUOMINEN<sup>2</sup>

<sup>1</sup> *NORDITA, Blegdamsvej 17, DK-2100 Copenhagen Ø, Denmark;*

<sup>2</sup> *Observatory and Astrophysics Laboratory, University of Helsinki, Tähtitorninmäki, SF-00130 Helsinki, Finland;*

<sup>3</sup> *Dept. of Mathematics, The University, Manchester M13 9PL, UK;*

<sup>4</sup> *Universitäts-Sternwarte, Getzmarlandstr. 11, D-3400 Göttingen, Fed. Rep. Germany*

(Received 21 February 1991; in final form 28 June 1991)

Nonlinear axisymmetric mean-field  $\alpha\Omega$ -type dynamos in spherical shells of conducting incompressible fluid are computed, with differential rotation being generated by the Reynolds stress of anisotropic turbulence ( $\Lambda$ -effect). The correlation time of the turbulence is assumed to be short compared with the rotation period. In this case the angular velocity tends to be constant on cylindrical surfaces as the Taylor number,  $Ta$ , is increased (cf. the Taylor-Proudman theorem). The only magnetic feedback mechanism considered is the Lorentz force of the mean magnetic field acting on the macroscale motions (Malkus-Proctor mechanism). The Elsasser number is in this case close to unity, but grows slowly as  $Ta^{1/2}$ . Restricting ourselves to strictly dipole-type magnetic fields we find for  $Ta = 10^4$ , magnetic cycles with migrating field belts close to the equator. For smaller Taylor numbers and only slightly supercritical  $\alpha$ -effect the magnetic field is steady and the  $\Omega$ -effect becomes unimportant for the generation of toroidal field from a poloidal one. However, magnetic cycles are still possible if the  $\alpha$ -effect is sufficiently strong. In this case the field is concentrated at high latitudes. Poloidal and toroidal fields can be in antiphase with equatorward field migration only when the angular velocity increases inwards and towards the poles. The energy of the mean magnetic field generated is usually less than the energy of the turbulent convective motions. The ratio between cycle period and rotational period can reach values of around fifty.

**KEY WORDS:** Hydromagnetics: mean-field dynamo, differential rotation, turbulence, Sun and stars; magnetic fields, stellar activity cycles.

### 1. INTRODUCTION

Simple kinematic mean-field  $\alpha\Omega$ -dynamos appear to be capable of explaining the basic features of the solar mean magnetic field, although the prescribed differential rotation may be unphysical in that it is not a consistent solution of the full dynamical problem. In the present paper we attempt to improve the mean-field  $\alpha\Omega$ -models by determining *simultaneously* both the magnetic field and the differential rotation.

In  $\alpha\Omega$ -type dynamos *two* induction processes are important in opposing the dissipation. The first arises from the turbulent e.m.f.  $\langle \mathbf{u}' \times \mathbf{B}' \rangle$ , leading to the  $\alpha$ -effect. The other includes the effects of large-scale flows such as differential rotation and meridional circulation. Both of these are essential for the  $\alpha\Omega$ -dynamo which is the standard explanation for stellar activity cycles. What is important here is that the

non-uniformity of the angular velocity also has its origin in the statistical properties of the turbulence. This has been formulated as the "A-effect" (Rüdiger, 1989, and references therein); its ancestry can be traced through the works of Lebedinski (1941), Wasylowski (1946), and Biermann (1951). In essence, the presence of anisotropy in the turbulent velocity field drives an angular momentum transport.

Thus a knowledge of the general turbulence field provides us with the input quantities  $\alpha$  and  $\Lambda$  in the dynamo equations, and so it is necessary to solve simultaneously both the dynamo and mean-field momentum equations, in order to construct a satisfactory model encompassing both the turbulent nature of the rotating convection zone and the resulting (large scale) mean-field structures.

In one way the present work is an extension of the  $\alpha^2$ -models of Malkus and Proctor (1975) and Proctor (1977), by including the generation of differential rotation by non-diffusive parts of the Reynolds stress tensor (i.e. the A-effect). In Malkus and Proctor's approach, non-uniform rotation also arises, but there it is only due to the feedback from the Lorentz force  $\langle \mathbf{J} \rangle \times \langle \mathbf{B} \rangle$  of the mean magnetic field. In contrast to this, here the differential rotation depends directly on the assumed properties of the hydrodynamic turbulence, via the mean-field momentum equation.

We can contrast our approach with that of Gilman and Miller (1981) and Glazmaier (1985), who solve directly the full equations, thus avoiding an *ad hoc* prescription of either an  $\alpha$ -effect or differential rotation. This involves a substantial computational effort because the timescale associated with the convective motions is short compared to the solar cycle period. At present this approach can only resolve giant cells, which may not be adequate (cf. Spruit *et al.*, 1990). In our formulation only the equations for the mean magnetic field and mean motions are considered.

The induced magnetic fields, both the fluctuations and the mean parts, feed back via the Lorentz force into the equations for both the mean and fluctuating motions. The simplest back-reaction is that of the large-scale Lorentz force,  $\langle \mathbf{J} \rangle \times \langle \mathbf{B} \rangle$ , which influences directly both the differential rotation profile and the meridional circulation. This effect has also been held responsible for causing the solar torsional oscillations.

The dominant feedback mechanism eventually determines the amplitude of the generated magnetic field. It is not yet clear, however, which of the various feedback mechanisms is the dominant one for stellar dynamos.  $\alpha^2$ -dynamo models with  $\alpha$ -quenching generate magnetic field strengths limited approximately by  $v_A \leq u$ , where  $v_A = [\langle \mathbf{B} \rangle] (\rho \mu_0)^{-1/2}$  is the Alfvén velocity of the mean magnetic field and  $u$ , the characteristic turbulent rms velocity. The resulting maximum possible field strength at the bottom of a mixing-length model of the solar convection zone reaches values of up to 5000 G. It has been argued that observations contradict this result (Durney *et al.*, 1990). If there is no reason for the appearance of a "dilution" factor in the  $\alpha$ -quenching expression one has to conclude that the observations do question the traditional feedback mechanism on  $\alpha$ . It is possible, however, that the inducing action of differential rotation might lead to super-equipartition values of the magnetic field strength. An interesting question is whether or not other nonlinear models can be constructed which allow magnetic fields exceeding the "turbulence equipartition value", given by  $v_A \approx u$ . In this paper the mean-field Lorentz force is the only feedback mechanism that we consider explicitly.

## 2. BASIC EQUATIONS

We consider here the initial value problem of a turbulent, incompressible, electrically conducting fluid with constant and uniform density,  $\rho$ , in a rotating shell with inner and outer radii  $r_0$  and  $R$ , respectively. We solve the hydromagnetic equations for the mean velocity and mean magnetic field, starting with a rigid rotation with angular velocity,  $\Omega_0$ , and a weak "seed" magnetic field.

We choose to work in an inertial frame of reference, because we expect that the variations of the angular velocity are of the order of the angular velocity itself and so there is no advantage in choosing a rotating frame. The assumption of incompressibility simplifies the numerical treatment of the equations considerably. Although this condition does not even approximately apply in stars, we feel that such models do nevertheless allow some understanding of the interaction between the mean motions and the mean magnetic field.

### 2.1 The Mean-field Equations

If microscopic transport processes are ignored, the evolution of the mean magnetic field and the mean velocity are governed by the dissipation-free induction and momentum equations:

$$\frac{\partial \langle \mathbf{B} \rangle}{\partial t} = \mathbf{V} \times (\langle \mathbf{u} \rangle \times \langle \mathbf{B} \rangle + \mathcal{E}), \quad (1)$$

$$\rho \frac{\partial \langle \mathbf{u} \rangle}{\partial t} = -\rho \langle \mathbf{u} \rangle \cdot \nabla \langle \mathbf{u} \rangle - \nabla p + \rho \mathbf{g} + \langle \mathbf{J} \rangle \times \langle \mathbf{B} \rangle - \nabla \cdot (\rho \mathcal{D} - \mathcal{B}), \quad (2)$$

where

$$\mathcal{E} = \langle \mathbf{u}' \times \mathbf{B} \rangle, \quad \mathcal{D}_{ij} = \langle u_i' u_j' \rangle, \quad \mathcal{B}_{ij} = \langle B_i' B_j' \rangle / \mu_0, \quad (3)$$

and

$$\mathbf{V} \cdot \langle \mathbf{B} \rangle = \nabla \cdot \langle \mathbf{u} \rangle = 0. \quad (4)$$

Here,  $p$  is the sum of gas and magnetic pressure,  $\rho$  density,  $\mathbf{g}$  gravity,  $\langle \mathbf{J} \rangle = \nabla \times \langle \mathbf{B} \rangle / \mu_0$  the electric current, and  $\mu_0$  the magnetic permeability. The system of equations has to be completed by boundary conditions for  $\langle \mathbf{u} \rangle$  and  $\langle \mathbf{B} \rangle$  (see Section 3.1).

### 2.2 Mean-field Transport Coefficients

We assume that the correlations  $\mathcal{D}$  and  $\mathcal{E}$  depend only linearly on the mean parts of the velocity and magnetic fields,  $\langle \mathbf{u} \rangle$  and  $\langle \mathbf{B} \rangle$ , respectively, and on their first

spatial derivatives, i.e.

$$\mathcal{E}_i = a_{ij} \langle B_j \rangle - b_{ijk} \partial_j \langle B_k \rangle, \quad (5)$$

$$\mathcal{Q}_{ij} = \Lambda_{ijk} \Omega_k - N_{ijk} \partial_k \langle u_i \rangle, \quad (6)$$

where the azimuthal velocity,  $\langle u_\phi \rangle$ , and the angular velocity,  $\Omega$ , are related via  $\langle u_\phi \rangle = (\Omega \times r)_\phi$ . The differential rotation in the Sun is much larger than variations of  $\Omega$  with the solar cycle. This would thus suggest that, in the Sun,  $\mathcal{Q}$  is less important than  $\mathcal{E}$ . We shall therefore neglect  $\mathcal{Q}$  in the present investigation. For simplicity we assume  $a_{ij}$ ,  $b_{ijk}$ , and  $N_{ijk}$  in (5) and (6) to be *isotropic* tensors:

$$a_{ij} = \alpha \delta_{ij}, \quad (7)$$

$$b_{ijk} = \eta_i \varepsilon_{ijk}, \quad (8)$$

$$N_{ijk} = \nu_i (\delta_{ik} \partial_j + \delta_{jk} \partial_i) + \mu_i \delta_{ij} \partial_k. \quad (9)$$

We assume further that  $\alpha$  takes the form  $\alpha = \tilde{\alpha} \cos \theta$ , where  $\theta$  is colatitude, and  $\tilde{\alpha}$  is taken here to be constant.  $\eta_i$  is a turbulent magnetic diffusivity and  $\nu_i$  a turbulent kinematic viscosity, both of which are also assumed to be constant, and  $\mu_i$  is a turbulent bulk viscosity which gives no contribution in the incompressible case. A non-vanishing tensor  $\Lambda_{ijk}$  cannot be constructed with isotropic tensors (Krause and Rüdiger, 1974). However, the stratification in a star gives a preferred direction,  $\hat{g}$ , and this causes the turbulence to be anisotropic. The simplest possible tensor which can be constructed using the unit vector in the radial direction,  $\hat{g}_i$ , is

$$\Lambda_{ijk} = \Lambda_V (\varepsilon_{ikp} \hat{g}_j + \varepsilon_{jkp} \hat{g}_i) \hat{g}_p. \quad (10)$$

Equation (10) only holds in the case of slow rotation with  $2\Omega_0 \tau_c \ll 1$ , where  $\tau_c$  is the correlation time of the turbulence. When the turbulence has approximately horizontal symmetry, the following estimate (Rüdiger, 1989) for the coefficient  $\Lambda_V$  may be useful:

$$\Lambda_V \approx 2\tau_c \langle u_\phi^2 \rangle - \langle u^2 \rangle. \quad (11)$$

This expression suggests that  $\Lambda_V$  is negative when the motions are mainly vertical. In this simplified form the  $\Lambda$ -effect strongly resembles the old formalism of "anisotropic viscosity" by Kippenhahn (1963). Kippenhahn favored  $\Lambda_V > 0$ , because in this case he reproduced the solar surface rotation law. However,  $\Lambda_V < 0$  would seem more probable, because we expect the turbulent motions to be stronger in the vertical than in the horizontal directions.

We mention here the possibility that, if  $\tau_c$  becomes comparable to the rotation period, the  $\Lambda$ -tensor may contain further terms, where  $\hat{\Omega}$  itself gives a preferred direction to the turbulence. For simplicity we shall not consider such effects here, but refer to Rüdiger (1989) and Brandenburg *et al.* (1990).

### 2.3 Non-dimensional Quantities

The ratio of the kinematic viscosity to the magnetic diffusivity is the magnetic Prandtl number,  $Pr_M = \nu_i/\eta_i$ . The Taylor number,  $Ta$ , is defined by

$$Ta = (2\Omega_0 R^2/\nu_i)^2, \quad (12)$$

where  $\Omega_0$  is the angular velocity of the initial, rigid, rotation. The strengths of the  $\alpha$ - and  $\Lambda$ -effects are characterized by the dimensionless numbers

$$C_\alpha = \tilde{\alpha} R/\eta_i, \quad \nu^{(0)} = \Lambda_V/\nu_i. \quad (13)$$

$C_\alpha > 0$  and  $\nu^{(0)} < 0$  is expected for the physically realistic situation of density decreasing with radius and a preferred vertical direction for the turbulence.

We now introduce non-dimensional variables by measuring length in units of the stellar radius  $R$ , i.e.  $[r] = R$ , time in magnetic diffusion times, i.e.  $[t] = R^2/\eta_i$ , and density in units of  $\rho$ . The units for the other variables are

$$[u] = \eta_i/R, \quad [B] = [u](\mu_0 \rho)^{1/2}, \quad [J] = [B]/(\mu_0 R). \quad (14)$$

### 3. THE NUMERICAL METHOD

In the following we omit for simplicity the parentheses and consider only averages of velocity and magnetic fields. We restrict ourselves to axisymmetric mean fields and write

$$\begin{aligned} u &= \varpi \Omega \hat{\phi} + \nabla \times (\psi \hat{\phi}), & B &= b \hat{\phi} + \nabla \times (a \hat{\phi}), \\ \omega &= \omega \hat{\phi} + \nabla \times (\varpi \Omega \hat{\phi}), & J &= j \hat{\phi} + \nabla \times (b \hat{\phi}), \end{aligned} \quad (15)$$

where  $\omega = \nabla \times u$  is the vorticity,  $\varpi = r \sin \theta$  the distance from the axis, and  $\hat{\phi}$  the unit vector in the  $\phi$ -direction. Below we refer also to the poloidal (or meridional) fields  $u_p = \nabla \times (\psi \hat{\phi})$  and  $B_p = \nabla \times (a \hat{\phi})$ . We can write (1) and (2) in the form

$$(\partial_t - D^2)a = \alpha b - \frac{1}{\varpi} u_p \cdot \nabla (\varpi a), \quad (16)$$

$$(\partial_t - D^2)b = \alpha j - \varpi u_p \cdot \nabla (b/\varpi) + \varpi B_p \cdot \nabla \Omega + \hat{\phi} \cdot (\nabla a \times B_p), \quad (17)$$

$$\begin{aligned} (\partial_t - Pr_M \nabla^2) \Omega &= -\frac{1}{\varpi^2} u_p \cdot \nabla (\varpi^2 \Omega) + \frac{1}{\varpi^2} B_p \cdot \nabla (\varpi b) \\ &\quad + Pr_M [\nabla \Omega \cdot \nabla \ln (\varpi^2) - \frac{1}{\varpi^2} \nabla \cdot (\varpi \Omega \Lambda)], \end{aligned} \quad (18)$$

$$(\partial_t - Pr_A D^2)\omega = 2\Omega\omega \frac{\partial\Omega}{\partial z} + \hat{\phi} \cdot \nabla \times \mathbf{f}, \quad (19)$$

where

$$\mathbf{f} = -\mathbf{u}_p \cdot \nabla \mathbf{u}_p + \mathbf{J} \times \mathbf{B} - \mathbf{V} \cdot \mathcal{B}^{(N)}, \quad (20)$$

Here,  $\mathcal{B}^{(N)}$  contains only terms from the  $\Lambda$ -effect with  $\mathcal{B}_i^{(N)} = (\hat{\phi} \cdot \Lambda_i + \hat{\phi} \cdot \Lambda_j)\Omega$ , where  $\Lambda = (\Lambda_r \sin \theta, 0, 0)$ . The linear operator  $D^2$  is defined by  $D^2 a = -\hat{\phi} \cdot \nabla \times (\nabla \times a \hat{\phi})$ . The function  $\psi$  has to be calculated by solving the equation

$$D^2 \psi = -\omega, \quad (21)$$

at every time step, and  $j$  is given by

$$j = -D^2 a. \quad (22)$$

### 3.1 The Boundary Conditions

We assume the sphere to be embedded in a vacuum, which implies

$$D^2 a = 0, \quad \text{and} \quad b = 0 \quad \text{for} \quad r > 1. \quad (23)$$

The interior and exterior solutions must be matched so that  $a$  and  $\partial a / \partial r$  are continuous on  $r = 1$ . This can be formulated as a non-local boundary condition for  $a$  on  $r = 1$ , which we handle using the matrix method described by Jepps (1975). At the inner boundary of the shell we assume a perfect conductor. This implies that the radial component of the magnetic field and the tangential component of the electric field both vanish on  $r = r_0$ , i.e.

$$\left. \begin{aligned} B_r &= 0 \\ \partial_r(B_\theta) + rB_\theta &= 0 \\ \partial_r(B_\phi) - rB_\phi &= 0 \end{aligned} \right\} \quad \text{on} \quad r = r_0. \quad (24)$$

In terms of  $a$  and  $b$  we then have

$$\left. \begin{aligned} a &= 0 \\ \partial_r(b) &= a \partial_r(a) \end{aligned} \right\} \quad \text{on} \quad r = r_0. \quad (25)$$

The third condition of (24) would lead to  $D^2 a + ab = 0$ , which is already satisfied by the differential equation (16). Like all model boundary conditions that ignore the complicated physical situation (overshoot etc.) at the base of the convection zone, this is merely a mathematically convenient condition, leading to an abrupt transition and an azimuthal surface current on  $r = r_0$ . Other simple choices of boundary condition are possible but have their own difficulties (see, e.g., Moss *et al.*, 1990).

Both boundaries are assumed to be stress free, i.e. the  $r - \theta$  and the  $r - \psi$  components of the total stress tensor must be continuous on the boundaries. Since the magnetic field itself is continuous on the boundary only the kinetic stress tensor needs to be considered. In a vacuum the components of the kinetic stress tensor vanish. In terms of  $\psi$ ,  $\omega$ , and  $\Omega$  we have then:

$$\left. \begin{aligned} r\partial_r(u_\theta/r) &\equiv \partial^2 \psi / \partial r^2 \equiv -\left(\frac{2}{r} \frac{\partial \psi}{\partial r} + \omega\right) = 0 \\ r\partial_r \Omega &= V^{(0)} \Omega \end{aligned} \right\} \quad \text{on} \quad r = r_0, 1, \quad \psi = 0 \quad (26)$$

The last equation makes it evident that the stress-free boundary condition already imposes a gradient of the angular velocity.

In this work we have restricted ourselves to strictly odd parity magnetic fields. We have therefore solved the equations only in one quadrant of the meridional plane, assuming  $a$  and  $\Omega$  to be even and  $b$ ,  $\psi$  and  $\omega$  to be odd about the equator. Our numerical scheme for the equations (16)–(19) employed a DuFort-Frankel scheme on a  $r$ ,  $\theta$  grid,  $0 \leq r \leq 1$ ,  $0 \leq \theta \leq \pi/2$ . Many of our calculations were performed with 21 meshpoints in each coordinate direction. In a number of cases we checked the solution using 41 or 63 points and typically found only small deviations from our standard resolution (but see Section 4.4). We also checked that decreasing the timestep did not significantly alter the solution. Since  $\psi$  does not vary greatly between time steps, it is convenient to solve (21) using a successive over-relaxation method (3–30 iterations are usually adequate).

## 4. RESULTS

We describe here the results of integrating (16)–(21) for a certain range of parameters  $Ta$ ,  $V^{(0)}$ , and  $C_T$ . We take  $r_0 = 0.7$  which corresponds to the position of the bottom of the solar convection zone. The magnetic Prandtl number has been put equal to unity.

### 4.1 Solutions in the Hydrodynamic Regime

We consider first the case without magnetic field ( $C_T = 0$ ) and investigate the motions in the rotating shell for different Taylor numbers,  $Ta$ , and different values of the parameter  $V^{(0)}$ . Starting from a rigidly rotating fluid as initial condition, i.e.  $\Omega = \Omega_0$  we find after some time a stationary solution. Note that the initially rigid rotation does not satisfy the boundary condition (26). A radial differential rotation is therefore quickly established; the faster the rotation rate, the more quickly a steady state is reached. In Table 1 we summarize the solutions found for various Taylor numbers and different values of the parameter  $V^{(0)}$ . These solutions are characterized by the surface angular velocity at the equator,  $\Omega_e$ , and at the pole,  $\Omega_p$ . The differences

Table 1. Summary of solutions in the hydrodynamic regime for different values of  $Ta$  and  $\nu^{(0)}$ 

$Ta$	$\nu^{(0)}$	$\Omega_e/\Omega_0$	$C_n$	$\Delta\Omega_e/\Omega_e$	$\Delta\Omega_p/\Omega_e$	$\Delta$	$ u_{\theta} _{\max}$	$ u_{\theta} _{\max}$
$10^2$	-2	0.769	-4	-1.04	-1.04	-0.00	0.02	0.06
$10^4$		0.765	-39	-1.02	-0.69	-0.29	1.7	4.8
$10^6$		0.651	-319	-0.98	-0.26	-1.29	15.5	30.6
$10^8$		0.675	-2700	-0.80	-0.07	-1.20	41.0	99.3
$10^2$	-1	0.884	-2	-0.43	-0.43	-0.00	0.01	0.0
$10^4$		0.857	-18	-0.42	-0.30	-0.21	0.79	2.0
$10^6$		0.805	-161	-0.41	-0.08	-0.83	2.11	8.7
$10^8$		0.811	-1460	-0.36	-0.02	-0.67	5.33	28.5
$10^2$	1	1.13	2	0.30	0.30	0.00	0.01	0.0
$10^4$		1.18	18	0.30	0.18	0.22	0.53	1.3
$10^6$		1.25	175	0.28	0.03	0.42	1.43	5.2
$10^8$		1.25	1690	0.27	0.01	0.44	2.11	16.0
$10^2$	2	1.25	3	0.51	0.50	0.01	0.01	0.03
$10^4$		1.39	36	0.51	0.26	0.39	0.80	2.2
$10^6$		1.51	372	0.49	0.05	0.69	2.78	7.7
$10^8$		1.54	3630	0.47	0.02	0.70	3.27	24.5

between the angular velocity at the top and the bottom of the shell are measured by  $\Delta\Omega_e$  and  $\Delta\Omega_p$ . The strength of the  $\Omega$ -effect, important later in the dynamo calculations, is measured by

$$C_n = Pr_M \Delta\Omega_e, \quad (27)$$

( $\Delta\Omega_e R^2/\eta$ , in dimensional units). We see from Table 1 that  $|C_n|$  increases with the Taylor number. As a rule of the thumb we may use  $C_n \approx (0.15 \dots 0.2)\nu^{(0)}Pr_M Ta^{1/2}$ . The relative radial differential rotation,  $|\Delta\Omega_e/\Omega_e|$ , decreases only slightly with  $Ta$ . The relative latitudinal differential rotation at the surface

$$\Delta = (\Omega_e - \Omega_p)/\Omega_e, \quad (28)$$

is, for  $Ta = 10^8$ , about 40% when  $\nu^{(0)} = +1$  and about 70% when  $\nu^{(0)} = +2$ . A negative value of  $\nu^{(0)}$  leads to a poleward increasing angular velocity. In the following we take  $\nu^{(0)} = +1$  or  $-1$ , as representative values.

The latitudinal differential rotation is generated from the meridional circulation by the nonlinear term  $u_p \cdot \nabla(\varpi^2 \Omega)$ . The meridional circulation itself is produced from the non-uniform rotation but also for a  $z$ -independent angular velocity,  $\Omega = \Omega(\varpi)$ . However, in both cases there would be still a meridional flow if the medium were non-adiabatically stratified and the thermodynamic equations were included (e.g. Moss and Vilhu, 1983). This is the analogue in a convective region of the well known Eddington-Sweet-Vogt circulation in rotating radiative envelopes (e.g. Sweet, 1950).

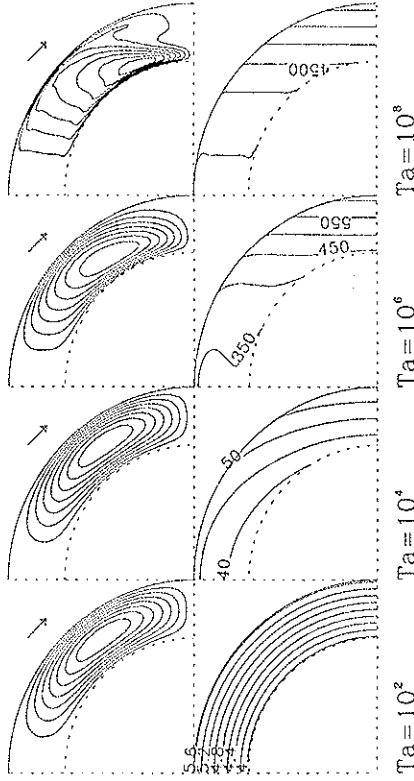


Figure 1. Streamlines of the meridional motion (upper row) and contours of constant  $\Omega$  (lower row) for various Taylor numbers.  $\nu^{(0)} = +1$ .

Figure 1 shows streamlines of the meridional motion and contours of constant angular velocity. Note that for faster rotation the streamlines become more and more elongated in the vertical direction and  $\Omega$  becomes almost constant on cylindrical surfaces (Taylor-Proudman theorem). As  $Ta \rightarrow \infty$ ,  $\Omega = \Omega(\varpi)$  is asymptotically satisfied. In this limit the momentum equation is satisfied by  $\partial\Omega/\partial z = 0$  and  $\psi = 0$ . The dependency of  $\Omega$  on  $\varpi$  is then given by  $\partial \ln \Omega / \partial \ln \varpi = \nu^{(0)}$ , from the boundary condition ( $2\phi$ )<sub>3</sub> applied at the equator. In higher latitudes deviations from strictly cylindrical  $\Omega$ -contours occur at the upper and lower boundary (cf. Figure 1). It should be noted that the  $\Omega$ -contours caused by the  $\nu^{(0)}$ -term are, in the viscous case, already cylindrical in the immediate vicinity of the equator. This is no longer true if higher order terms in the  $\Lambda$ -effect are included. It might be expected that these terms could delay somewhat the onset of the Taylor-Proudman effect, but this does not seem to be the case, see Brandenburg *et al.* (1990).

When the isolines of  $\Omega$  lie on cylinders the centrifugal force can always be expressed as the gradient of a potential so that it can essentially be balanced by the pressure gradient alone—without any circulation. In fact, Köhler (1970) found a maximum of the meridional flow velocity for  $Ta \approx 3 \times 10^7$ . However, from Table 1 we see that the values for  $|u_{\theta}|_{\max}$  and  $|u_{\theta}|_{\max}$  always increase with  $Ta$ . This is an artifact of the normalization chosen here. The dimensional meridional velocity scales with  $\eta/R$ , see (14), and it indeed decreases for large values of  $Ta$ , because  $\eta_i$  decreases faster than the increase of  $|u_{\theta}|_{\max}$  assuming  $\Omega_0$  and  $R$  to be held constant.

Spherical three-dimensional models by Gilman (1977), in which differential rotation is automatically generated by Reynolds stresses from the large-scale thermal convection, show cylindrical  $\Omega$  contours in lower latitudes. Equatorial acceleration

occurs only if the Rayleigh number is not too large, otherwise the profile at lower latitudes is reversed. The Taylor number in Gilman's models corresponds with our definition to  $6 \times 10^7$ . The meridional circulation in this model is always poleward in lower latitudes, which seems to be in disagreement with our results, the results for the angular velocity are in approximate agreement with ours.

#### 4.2 Solutions in the Hydromagnetic Regime

We now consider solutions for supercritical values of  $C_\alpha$ . Starting from a small initial perturbation in  $\mathbf{B}$  and a rigid rotation, a differential rotation is first established, before the growth of the magnetic field into the nonlinear regime. We computed models for different values of  $Ta$ ,  $\nu^{(0)}$ , and  $C_\alpha$ . The results are summarized in Table 2. The magnetic field is characterized by the total energy (in dimensionless units) of the mean magnetic field inside the convection zone,

$$E_M = \frac{1}{2} \int_{CZ} |\mathbf{B}|^2 dV, \quad (29)$$

and by the ratio of the energy of mean poloidal and mean toroidal field,  $E_p/E_t$ . The other quantities, characterizing the motions, are the same as in the previous section. For oscillatory solutions  $T_{cyc} = 2\pi/\Omega_{cyc}$  denotes the period of the magnetic cycle.

For slightly supercritical values of  $C_\alpha$  we find steady solutions for  $Ta \leq 10^6$  and oscillatory solutions for  $Ta = 10^8$ . This behavior can change for larger values of  $C_\alpha$ . For  $Ta \leq 10^6$  the magnetic field is concentrated at high latitudes with  $E_p/E_t = O(1)$ ,

Table 2 Summary of solutions in the hydrodynamic regime for various values of  $Ta$  with  $\nu^{(0)} = \pm 1$

$Ta$	$\nu^{(0)}$	$C_\alpha$	$\lg E_M$	$E_p/E_t$	$C_\alpha$	$T_{cyc}$
$10^4$	-1	15	1.37	1.57	-18	steady
	-1	16	1.65	1.71	-18	steady
	+1	16	1.65	1.38	+18	steady
	+1	20	2.17...2.73	1.02...1.57	+18	0.28
	-1	10	2.54	0.22	-165	steady
$10^6$	-1	12	2.77	0.42	-165	steady
	-1	14	2.94	0.81	-165	steady
	-1	15	3.03	1.05	-163	steady
	-1	16	3.11	1.29	-161	steady
	-1	20	3.38	2.01	-152	steady
	+1	18	1.85	1.31	+176	steady
	+1	20	1.71...2.35	0.94...2.08	+176	0.15
	+1	25	2.57...3.32	0.80...2.98	+176	0.055
	-1	4	3.49...3.82	0.004...0.007	-1490...-1500	0.064
	-1	6	4.18...4.45	0.009...0.015	-1230...-1330	0.058
$10^8$	-1	10	4.28...4.57	0.029...0.048	-830...-1090	0.066
	-1	20	4.60	1.38	-630	steady
	+1	6	4.08...4.19	0.021...0.032	-1580...-1560	0.041

whereas for  $Ta = 10^8$  there is a dominant toroidal field close to the equator. We discuss first the solutions for  $Ta = 10^8$  (Section 4.3). For  $Ta \leq 10^6$  and sufficiently supercritical values of  $C_\alpha$  there is another class of oscillatory solutions, that are discussed in Section 4.4.

#### 4.3 Magnetic Cycles

Oscillatory solutions (magnetic cycles) occur for  $Ta = 10^8$ . The cycle period is  $T_{cyc} = 0.04...0.07$  (depending on the sign of  $\nu^{(0)}$ ). The ratio of cycle period to rotation period is  $T_{cyc}/T_{rot} = T_{cyc} P_T / Ta^{1/2} / (4\pi) = 30...50$ . If solar values,  $\nu_r = \eta_r = 5 \times 10^{12} \text{ cm}^2/\text{s}$ , where applied, then this Taylor number would correspond to a rotation period of about 15 days and the cycle period to 1...2 years. Note that the total energy is nearly independent of  $C_\alpha$ . There is only an increase of  $E_p/E_t$  with  $C_\alpha$  indicating that energy goes more into the poloidal field than into the toroidal.

Snapshots showing the evolution of magnetic and velocity fields for a dynamo with  $Ta = 10^8$ ,  $C_\alpha = 10$ , and  $\nu^{(0)} = -1$  are given in Figure 2. There are always two

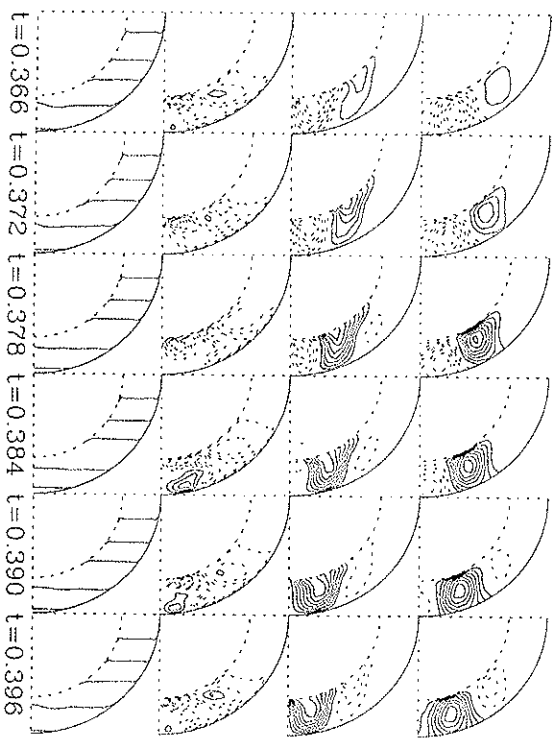


Figure 2 Evolution of the magnetic fields and motions for a dynamo with high Taylor number ( $Ta = 10^8$ ,  $C_\alpha = 10$  and  $\nu^{(0)} = -1$ ). In the first row are the magnetic field lines of the poloidal field, in the second row contours of constant toroidal field, in the third row streamlines of the meridional motion, and in the last row contours of constant angular velocity. Dotted lines denote negative values (second row) or counterclockwise circulation (first and third row).

magnetic field belts migrating equatorwards. Note also that they are strongly concentrated to the bottom of the convection zone. The meridional flow is clearly affected by the magnetic field. Thin clockwise rotating rolls are superimposed on the "background" circulation pattern. These rolls are located between the magnetic field belts and also migrate equatorwards. The time dependent field geometry of the oscillatory solutions is conveniently represented by butterfly diagrams showing the latitudinal and temporal evolution of the magnetic field ( $B_r$ - and  $B_\theta$ -components) in a  $\theta$ - $t$  map. The butterfly diagrams for  $B_r$  and  $B_\theta$  for the same model as in Figure 2 are given in Figure 3.  $B_r$  is taken at  $r=1$  and  $B_\theta$  at  $r=1-\Delta r$ , where  $\Delta r$  is the mesh width (here 0.0375). Note that fields are strongly concentrated to the equator.

The migration direction and the phase relations are as expected (cf. Stix, 1976; Yoshimura, 1976). Field belts migrate equatorward for  $C_\alpha \nu^{(0)} < 0$  and poleward for  $C_\alpha \nu^{(0)} > 0$ .  $B_r$ - and  $B_\theta$ -fields are in phase when  $C_\alpha < 0$  and in antiphase when  $C_\alpha > 0$ . The general solar field geometry is obtained for  $C_\alpha > 0$  and  $\nu^{(0)} < 0$ . These signs of both quantities were also favored in Section 2.3. However the angular velocity is then increasing not only inwards, but also towards the poles. The problem of reproducing both the solar field geometry and the differential rotation contours leads to the well known "dynamo dilemma" (Parker, 1987).

Three-dimensional models of convective dynamo action in spherical shells by

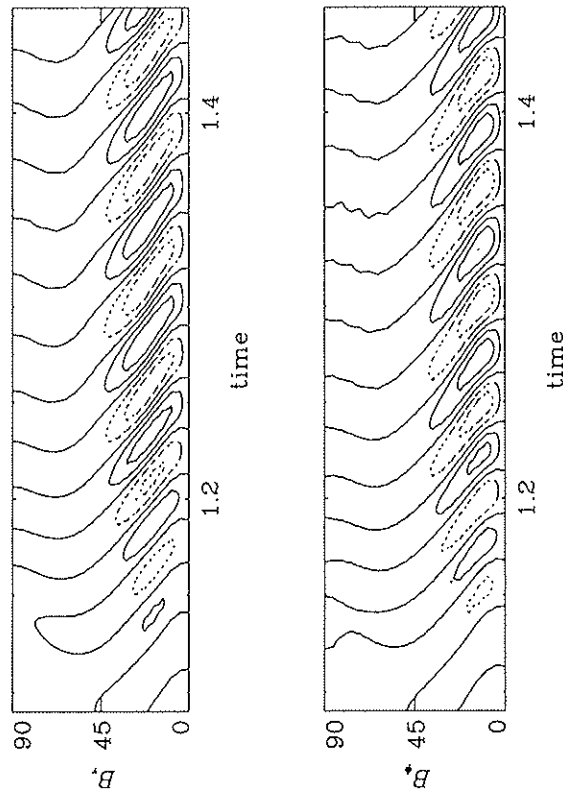


Figure 3 Butterfly diagrams for the  $B_r$ - and  $B_\theta$ -components for the model of Figure 2. Note that the fields are out of phase and concentrated close to the equator.

Gilman (1983) show many properties similar to ours: The magnetic cycle period is one order of magnitude shorter than that of the Sun, dynamo action becomes non-oscillatory for large values of  $Pr_M$  (large conductivity, large  $C_\alpha$ ), and the differential rotation is substantially quenched by the Lorentz force of the dynamo-generated magnetic fields.

#### 4.4 Magnetic Relaxation Oscillations

Here we consider  $\nu^{(0)} = +1$ . For  $C_\alpha \geq 20$  oscillations are possible even with small Taylor numbers ( $Ta = 10^4$ ). The magnetic field is then concentrated at high latitudes. The evolution of magnetic fields and motions for this dynamo are shown as a butterfly diagram in Figure 4. The different nature of this type of magnetic cycles compared with traditional  $\alpha\Omega$ -dynamoes becomes evident by considering the migration direction of magnetic-field belts, which is equatorwards although  $C_\alpha \nu^{(0)} > 0$  (and thus  $\alpha\partial\Omega/\partial r > 0$  in the northern hemisphere). Furthermore  $B_r$  and  $B_\theta$  are nearly in phase although  $C_\alpha > 0$ . Also there is no polar branch. Clearly, this type of dynamo with its nonlinear oscillations is of a quite different nature to traditional  $\alpha\Omega$ -dynamoes.

For large values of  $C_\alpha$  (e.g. 25) an irregular time behavior occurred when using the standard resolution of  $21 \times 21$  mesh points. Using better resolution (e.g.  $63^2$  mesh points) we found that the oscillations were in fact regular.

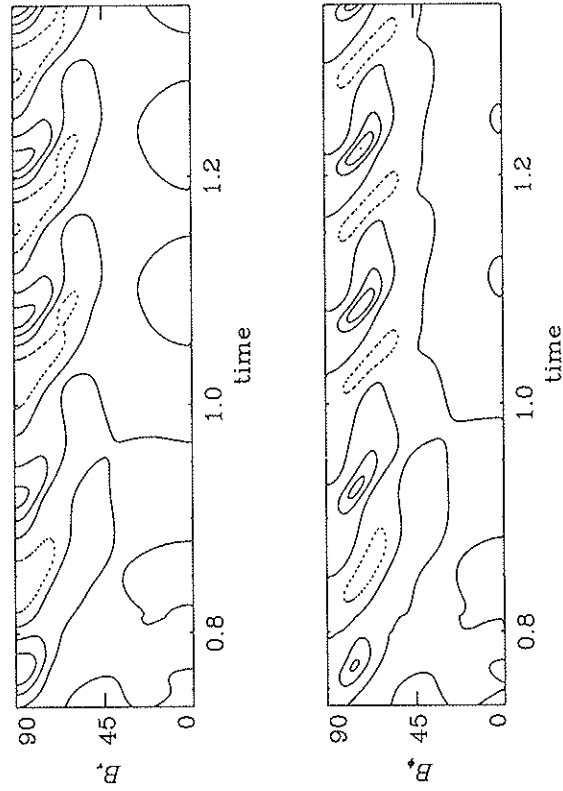


Figure 4 Butterfly diagrams for the  $B_r$ - and  $B_\theta$ -components for a model with small Taylor number ( $Ta = 10^4$ ,  $C_\alpha = 20$  and  $\nu^{(0)} = +1$ ).

## 4.5 The Role of Meridional Circulation

The meridional circulation also plays a significant role for the dynamo: in Roberts and Stix (1972) it inhibited the dynamo action. However, the strength of this effect was treated there as a free parameter. In contrast, Roberts (1989) presented a model in which a more consistent meridional flow supported the dynamo. In our present models meridional circulation is self-consistently included. In Table 3 we have computed models where we enforced  $u_p = 0$  in the dynamo equations. By comparison with Table 2 we find that for  $Ta \leq 10^6$  meridional circulation enhances dynamo action if  $\nu^{(0)} < 0$  (poleward circulation), but inhibits dynamo action if  $\nu^{(0)} > 0$  (equatorward circulation). The model presented by Roberts (1989) had negative shear and agrees with our case with  $\nu^{(0)} < 0$ . For  $Ta = 10^8$  meridional circulation always suppresses dynamo action. In the absence of meridional circulation the solutions are also oscillatory for  $Ta = 10^6$  and marginal values of  $C_a$ .

4.6 The Transition from  $\alpha^2$  to  $\alpha\Omega$  Dynamos

A standard approximation in  $\alpha\Omega$ -dynamo theory is to neglect the  $\alpha$ -effect for the generation of toroidal field from a poloidal one. For axisymmetric magnetic fields this is justified, if  $C_a \gg C_\alpha$ . We have checked this for our models by neglecting the  $\alpha$ -effect in (17) (see Table 6). It turns out that the  $\alpha\Omega$ -dynamo approximation is a reasonable one for  $Ta = 10^8$ , but for  $Ta = 10^6$  the results are seriously in error.

**Table 3** Summary of solutions with meridional circulation suppressed. By comparison with Table 2, meridional circulation is seen to enhance dynamo action if  $\nu^{(0)} < 0$  (+ sign in the last column), but to inhibit dynamo action if  $\nu^{(0)} > 0$  (— sign in the last column). An asterisk denotes solutions that are not excited in the presence of meridional circulation

$Ta$	$\nu^{(0)}$	$C_a$	$\lg E_\omega$	$E_p/E_i$	$C_\alpha$	$T_{\text{osc}}$	Result
$10^4$	—1	15	0.94	1.59	—19	steady	+
	—1	16	1.55	1.68	—19	steady	+
	+1	16	1.88	1.41	+17	steady	—
$10^6$	—1	15	2.41...2.50	0.31...0.43	—188...—193	0.096	+
	—1	16	2.75...2.87	0.50...0.69	—186...—193	0.110	+
	+1	16	2.39...2.41	0.68...0.81	+170	0.104	—*
	+1	18	2.72...2.90	0.87...0.97	+171	0.100	—
	—1	3	3.89...4.05	0.004...0.006	—1860...—1890	0.052	—*
$10^8$	—1	4	4.31...4.47	0.008...0.011	—1770...—1840	0.052	—
	—1	6	4.38...4.57	0.017...0.026	—1580...—1710	0.052	—
	—1	10	4.34...4.56	0.045...0.082	—1380...—1530	0.052	—
	+1	4	3.92...3.95	0.026...0.028	+1704	0.050	—
	+1	6	4.17...4.21	0.040...0.046	+1701	0.048	—

## 5. FEEDBACK MECHANISMS

## 5.1 The Amplitude of the Dynamo

The nonlinear feedback via the Lorentz forces determines the amplitude of the generated magnetic field. When the term  $\mathbf{j} \times \mathbf{B}$  was neglected in (20) we found the energy to be approximately unchanged. From this we conclude that it is the term  $\mathbf{B}_p \cdot \nabla(\omega b)$  in (18) that limits the magnetic field strength in our models. In order to see which terms in (18) balance the toroidal Lorentz force we compare  $\mathbf{B}_p \cdot \nabla(\omega b)$  both with  $\mathbf{u}_p \cdot \nabla(\omega^2 \Omega)$  and with  $Pr_A \nabla \cdot (\omega^2 \nabla \Omega - \omega \Omega \mathbf{A})$  (see Figure 5). It turns out that, away from the polar regions, the toroidal Lorentz force is balanced primarily by the inertial term  $\mathbf{u}_p \cdot \nabla(\omega^2 \Omega)$ , which also includes the Coriolis force in our frame of reference. This feedback is sometimes called the Malkus-Proctor mechanism. The quantity characterizing this balance is

$$\frac{|\mathbf{B}_p \cdot \nabla(\omega b)|}{|\mathbf{u}_p \cdot \nabla(\omega^2 \Omega)|}. \quad (30)$$

This ratio may be estimated by the Elsasser number  $\sigma |\mathbf{B}_p| |\mathbf{B}_\Omega| / (2\Omega \rho)$  (Roberts, 1988),

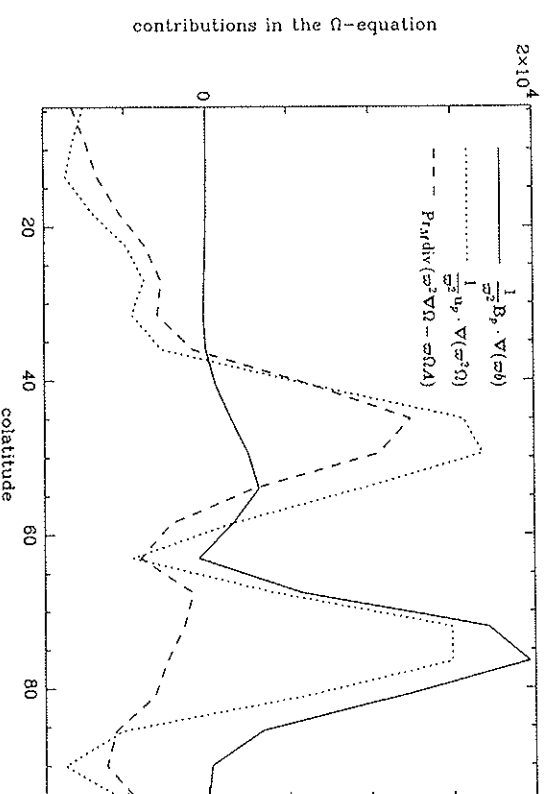


**Figure 5** Contributions to  $\partial\Omega/\partial t$  along a meridian of radius 0.91. Note that the Lorentz force  $(1/\omega^2)\mathbf{B}_p \cdot \nabla(\omega b)$  (solid line) is balanced predominantly by  $(1/\omega^2)\mathbf{u}_p \cdot \nabla(\omega^2 \Omega)$  (dotted line), whilst  $(Pr_A \nabla \cdot (\omega^2 \nabla \Omega - \omega \Omega \mathbf{A}))$  (dashed line) has a local extremum that in turn coincides with  $(1/\omega^2)\mathbf{u}_p \cdot \nabla(\omega^2 \Omega)$ .



in our runs. The peak values of  $v_M/u_c$  are typically larger by a factor of about five than our estimated values (35) and so can approach unity. In this case the neglect of effects such as  $\alpha$ -quenching becomes questionable. In the lower panel of Figure 6 we have also plotted  $El(Ta)$ . We find  $El=O(1)$  for large values of  $Ta$ . We have compared these results with those obtained for both  $Pr_M=0.1$  and  $Pr_M=10$ , but the same value of  $TaPr_M^2$  (see Table 5). We found that the magnetic energy increases with  $Pr_M$ . In Table 5 we have also given the Elsasser numbers [see (31)]. The table shows that  $El/Pr_M$  varies much less with  $Pr_M$  than  $El$ . This behavior can partly be explained by the decreasing magnitude of  $u_p$  with increasing Taylor number (see Section 4.1). In (30)  $u_p$  scales roughly with  $v_c/R$  so that (30) can be estimated as  $|B_p||B_z|/R/(v_c 2\Omega\rho)$ .

### 5.3 The Magnitude of $\alpha$

There is another important point concerning the magnitude of  $C_\alpha$ . Using again (32) and (33) we find

$$C_\alpha \approx \Omega R/\eta \approx 3\Omega R/u_c. \quad (36)$$

In solar-type stars this ratio grows from the order unity in the surface region ( $u_c = 1 \dots 5$  km/s) to order 100 near the bottom of the convection zone ( $u_c = 20 \dots 100$  m/s). Trial computations in which  $\alpha$  is prescribed to vary in such a way suggest that it is  $\max(\alpha)$  that determines the critical dynamo number. Together with the results in Table 2 the estimate in (36) leads to values that are less than 20 times supercritical, and does *not* confirm the often quoted dilemma of  $\alpha$  being supercritical by about two orders of magnitude in the Sun. If we attempt, however, to force the magnetic cycle period to 22 years by reducing the value of  $\eta$  to about  $0.03u_c l$  then we do obtain values for  $C_\alpha$  that certainly are highly supercritical. The effective value of  $\alpha$  may also be strongly reduced by the intermittency of the magnetic field.

**Table 5** Comparison of the Elsasser numbers for three different values of  $Pr_M$ . For  $Pr_M=0.1$  we used a resolution of  $41 \times 41$  meshpoints and for larger values of  $Pr_M$  the standard resolution of  $21 \times 21$  meshpoints. For  $Pr_M=0.1$  we used  $C_\alpha=10$ , because the field decayed for  $C_\alpha=8.9$

$Pr_M$	$Ta$	$C_\alpha$	$\lg E_M$	$E_p/E_c$	$C_\alpha$	$El$	$El/Pr_M$
0.1	$2 \cdot 10^9$	10.0	2.99	0.151	-511	0.074	0.74
1	$2 \cdot 10^7$	8.9	3.89	0.067	-619	0.42	0.42
10	$2 \cdot 10^5$	8.9	4.70	0.103	-766	3.2	0.32

**Table 6** Results for the case where the  $\alpha$ -effect is neglected in (17)

$Ta$	$\gamma^{(0)}$	$C_\alpha$	$\lg E_M$	$E_p/E_c$	$C_\alpha$	$T_{osc}$
$10^6$	-1	100	1.89 ... 1.91	2.23 ... 2.75	-158	0.028
	+1	80	1.50 ... 1.52	2.19 ... 3.00	+175	0.080
$10^8$	-1	6	4.09 ... 4.33	0.009 ... 0.014	-1300 ... -1370	0.053

## 6. CONCLUSIONS

The models presented here clearly have an important advantage over purely kinematic models. Differential rotation is not prescribed in a completely *ad hoc* manner as in other investigations of nonlinear  $\alpha\Omega$ -dynamics (Jepps, 1975; Ivanova and Ruzmaikin, 1977; Schmitt and Schüssler, 1989), but the variation of  $\Omega$  from the magnetic feedback is taken into account.

However, our model is still very simplified. For example the density is constant and thermodynamics are omitted. Also the input quantities,  $\alpha$  and  $\Lambda$ , are assumed to be constant. The intermittent nature of magnetic fields under conditions of high magnetic Reynolds numbers leading, for example, to buoyancy losses, is neglected. However, this work may be regarded as an elementary investigation of  $\alpha$ -effect dynamos with generation of differential rotation and meridional circulation employing the  $\Lambda$ -effect formalism for slowly rotating stars ( $2\Omega\tau_c \ll 1$ ). We have not attempted here to construct a model which closely reproduces the solar cycle but note that all of these models fail in some way to reproduce the gross properties of the solar cycle (see also Brandenburg *et al.*, 1990). The inclusion of compressibility together with overshoot layer effects and/or differential rotation generators concentrated near the bottom of the convection zone all offer possibilities for future work.

Our basic result is that magnetic cycles for weakly supercritical  $\alpha$  are possible only for large Taylor numbers,  $O(10^8)$ , unless the magnetic Prandtl number is substantially larger than unity. Certainly, for modelling the Sun the horizontal components of the  $\Lambda$ -tensor should be taken into account in order to seek a negative gradient of the radial differential rotation and simultaneously an equatorward increasing differential rotation. This can lead to disk-shaped  $\Omega$ -contours, which are in better accordance with recent results of helioseismology than cylindrical  $\Omega$ -contours. However, this seems to be possible only for Taylor numbers which are not too large, because otherwise cylindrical  $\Omega$ -contours inevitably occur (Taylor-Proudman theorem). These results are consistent with those from three-dimensional models of both incompressible (Gilman, 1977) and compressible (Gilman and Miller, 1986) convection in rotating spherical shells. Furthermore, our calculations are still subject to the "dynamo dilemma", in which correct solar magnetic field properties can only be achieved with an angular velocity that increases inwards.

Observations of slowly rotating stars can, in principle, reveal the dependence of the generated mean-field magnetic energy on the basic rotation rate. Thus we need predictions for this function from various dynamo models. What we find from our current computations is a rather steep dependence of the magnetic energy  $E_M$  on the Taylor number  $Ta$ . Since magnetic braking causes Taylor numbers to decrease during the evolution of a single star, the slope of the  $E_M(Ta)$ -relation might become an observational constraint on dynamo models.

## References

- Biermann, L., "Bemerkungen über das Rotationsgesetz in irdischen und stellaren Instabilitätszonen," *Zeitschr. f. Astrophys.* 28, 304-309 (1951).
- Brandenburg, A., Moss, D., Rüdiger, G. and Tuominen, I., "The nonlinear solar dynamo and differential rotation: A Taylor number puzzle," *Solar Phys.* 128, 243-251 (1990).

where  $\sigma = l/(\mu_0 \eta)$  is the turbulent conductivity and  $|B_p|$  and  $|B|$  are typical values for the poloidal and toroidal magnetic field. We define here a global Elsasser number as

$$El = (E_p/E_t) Ta^{1/2} Pr_M^{-1}. \quad (31)$$

where  $E_p$  and  $E_t$  are the magnetic energies of the poloidal and toroidal magnetic fields. Roberts argues that the Elsasser number is the relevant parameter governing the field strength of a dynamo on the so-called strong-field branch.

It should be remembered that in a complete physical model effects neglected here, such as feedback from small scale magnetic fields,  $\alpha$ - and  $\Lambda$ -quenching, magnetic buoyancy, may also be important or even dominant.

We are interested in the dependence of the magnetic energy on the Taylor number. In general, the  $\alpha$ -effect cannot be considered as independent of the angular velocity of the star. Using  $\alpha \approx \Omega l \cos \theta$  (cf. Steenbeck *et al.*, 1966), where  $l$  is the correlation length of the turbulence (typically the density scale height), we find

$$C_\alpha = \frac{1}{2} \xi Pr_M Ta^{1/2}, \quad (32)$$

where  $\xi = l/R$  and characterizes properties of stellar turbulence. In Table 4 we have summarized dynamo solutions for  $\xi = 0.002$  and  $\xi = 0.004$  as a function of  $Ta$ . The models with  $\xi = 0.002$  are oscillatory whilst those with  $\xi = 0.004$  are normally steady, but oscillate for a small range of  $Ta$ . Note that  $E_p/E_t$  increases and  $C_\alpha$  decreases with  $Ta$ . In the case  $\xi = 0.002$  increases with  $Ta$  for  $Ta \gtrsim 7 \cdot 10^7$ .

Table 4 Magnetic energy for different values of  $Ta$  and  $\xi$ .  $\nu^{(0)} = -1$ . Note that for  $\xi = 4 \cdot 10^{-3}$  there are both steady and oscillatory solutions

$\xi$	$Ta$	$C_\alpha$	$\lg E_M$	$E_p/E_t$	$C_\alpha$	$T_{\text{osc}}$
$2 \cdot 10^{-3}$	$5 \cdot 10^7$	7.1	3.75...4.04	0.013...0.022	-964...-1001	0.061
	$7 \cdot 10^7$	8.4	4.11...4.33	0.017...0.028	-978...-1080	0.050
	$8 \cdot 10^7$	8.9	4.19...4.46	0.019...0.031	-918...-1048	0.061
	$1 \cdot 10^8$	10.0	4.28...4.57	0.029...0.048	-828...-1091	0.066
	$1.5 \cdot 10^8$	12.2	4.43...4.70	0.052...0.085	-731...-1150	0.084
$4 \cdot 10^{-3}$	$2 \cdot 10^7$	8.9	2.92...3.28	0.021...0.038	-673...-675	0.070
	$3 \cdot 10^7$	11.0	3.75...4.05	0.034...0.060	-651...-717	0.072
	$1 \cdot 10^7$	6.3	3.49	0.039	-481	steady
	$2 \cdot 10^7$	8.9	3.89	0.067	-610	steady
	$3 \cdot 10^7$	11.0	4.06	0.115	-673	steady
$4 \cdot 10^{-3}$	$5 \cdot 10^7$	14.1	4.24	0.308	-686	steady
	$7 \cdot 10^7$	16.7	4.39	0.684	-662	steady
	$1 \cdot 10^8$	20.0	4.60	1.38	-630	steady
	$1.5 \cdot 10^8$	24.5	4.81	1.73	-620	steady
	$2 \cdot 10^8$	28.0	4.97	2.40	-593	steady

### 5.2 The Equipartition Problem

An important question in stellar dynamo theory is whether the magnetic energy can exceed the equipartition value given by  $v_A/u_c = 1$ . We assume for the following

$$\eta_i = \frac{1}{3} u_i l_i, \quad (33)$$

and estimate the magnetic field using the global magnetic energy  $E_M \approx 4\pi d^3 |B|^2$ , where  $d$  is the fractional depth of the convection zone. We obtain with (14)

$$E_M \approx 18\pi d \frac{v_A^2}{u_i^2} \xi^{-2}. \quad (34)$$

For  $d = 0.3$  we have

$$\frac{v_A}{u_i} \approx 0.24 \xi E_M^{1/2}. \quad (35)$$

In Figure 6 (upper panel) we have plotted  $v_A/u_i$  as a function of  $Ta$  for two models in Table 4. Note that  $v_A/u_i$  is approximately proportional to  $Ta^{1/2}$ , i.e. the energy of the mean magnetic field grows proportionally to  $Ta$ . Over-equipartition is not reached

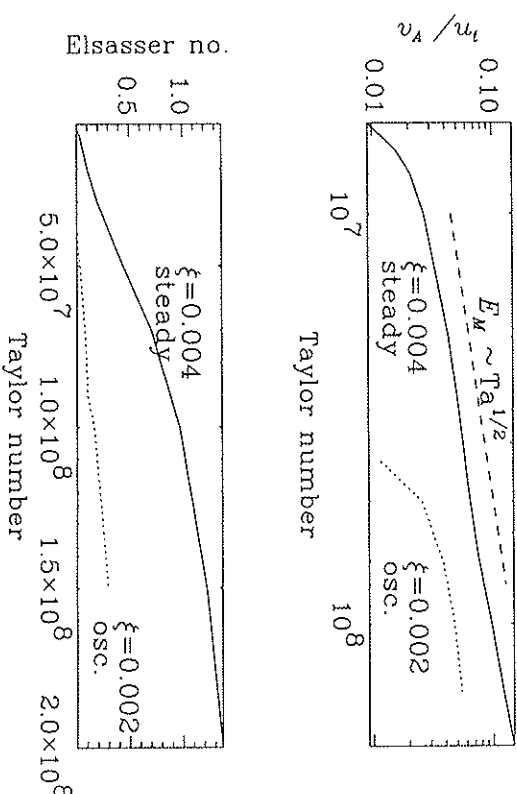


Figure 6 Equipartition value,  $v_A/u_i$ , (upper panel) and Elsasser number,  $El$ , (lower panel) versus  $Ta$  for two values of  $\xi$  for two models of Table 4.

- Durney, B. R., De Young, D. S. and Passot, T. P., "On the generation of the solar magnetic field in a region of weak buoyancy," *Astrophys. J.* **362**, 709-721 (1990).
- Gilman, P. A., "Nonlinear dynamics of Boussinesq convection in a deep rotating shell. I," *Geophys. Astrophys. Fluid Dynam.* **8**, 93-135 (1977).
- Gilman, P. A., "Dynamically consistent nonlinear dynamos driven by convection in a rotating spherical shell. II. Dynamos with cycles and strong feedbacks," *Astrophys. J. Suppl.* **53**, 243-268 (1983).
- Gilman, P. A. and Miller, J., "Dynamically consistent non-linear dynamos driven by convection in a rotating spherical shell," *Astrophys. J. Suppl.* **46**, 211-238 (1981).
- Gilman, P. A. and Miller, J., "Nonlinear convection of a compressible fluid in a rotating spherical shell," *Astrophys. J. Suppl.* **61**, 585-608 (1986).
- Glatzmaier, G. A., "Numerical simulations of stellar convective dynamos. II. Field propagation in the convection zone," *Astrophys. J.* **291**, 300-307 (1985).
- Ivanova, T. S. and Ruzmaikin, A. A., "A nonlinear magnetohydrodynamic model of the solar dynamo," *Sov. Astron.* **21**, 479-483 (1977).
- Jepps, S. A., "Numerical models of hydromagnetic dynamos," *J. Fluid Mech.* **67**, 625-646 (1975).
- Kippenhahn, R., "Differential rotation in stars with convective envelopes," *Astrophys. J.* **137**, 664-678 (1963).
- Köhler, H., "Differential rotation caused by anisotropic turbulent viscosity," *Solar Phys.* **13**, 3-18 (1970).
- Krause, F. and Rüdiger, G., "On the Reynolds stresses in mean-field hydrodynamics I. Incompressible homogeneous isotropic turbulence," *Astron. Nachr.* **295**, 93-99 (1974).
- Lebedinski, A. I., "Rotation of the Sun," *Astron. Zh.* **19**, 10-25 (1941).
- Maikus, W. V. R. and Proctor, M. R. E., "The macrodynamics of  $\alpha$ -effect dynamos in rotating fluids," *J. Fluid Mech.* **67**, 417-443 (1975).
- Moss, D. and Vilhu, O., "Models of stellar differential rotation on the lower main sequence," *Astron. Astrophys.* **119**, 47-53 (1983).
- Moss, D., Tuominen, I. and Brandenburg, A., "Buoyancy limited thin shell dynamos," *Astron. Astrophys.* **240**, 142-149 (1990).
- Parker, E. N., "The dynamo dilemma," *Solar Phys.* **110**, 11-21 (1987).
- Proctor, M. R. E., "Numerical solutions of nonlinear  $\alpha$ -effect dynamo equations," *J. Fluid Mech.* **80**, 769-784 (1977).
- Roberts, P. H., "Future of geodynamo theory," *Geophys. Astrophys. Fluid Dynam.* **42**, 3-31 (1988).
- Roberts, P. H., "From Taylor state to model-Z," *Geophys. Astrophys. Fluid Dynam.* **49**, 143-160 (1989).
- Roberts, P. H. and Stix, M., " $\alpha$ -effect dynamos, by the Bullard-Gellman Formalism," *Astron. Astrophys.* **18**, 453-466 (1972).
- Rüdiger, G., *Differential rotation and stellar convection: Sun and solar-type stars*, Gordon & Breach, New York (1989).
- Schmitt, D. and Schüssler, M., "Non-linear dynamos. I. One-dimensional model of a thin layer dynamo," *Astron. Astrophys.* **223**, 343-351 (1989).
- Spruit, H.-C., Nordlund, Å. and Title, A. M., "Solar convection," *Ann. Rev. Astron. Astrophys.* **28**, 263-301 (1990).
- Steenbeck, M., Krause, F. and Rädler, K.-H., "Berechnung der mittleren Lorentz-Feldstärke  $\mathbf{v} \times \mathbf{B}$  für ein elektrisch leitendes Medium in turbulenter, durch Coriolis-Kräfte beeinflusster Bewegung," *Z. Naturforsch.* **21a**, 369-376 (1966).
- Stix, M., "Differential rotation and the solar dynamo," *Astron. Astrophys.* **47**, 243-254 (1976).
- Sweet, P. A., "The importance of rotation in stellar evolution," *Mon. Not. R. astr. Soc.* **110**, 548-558 (1950).
- Wasylunski, J., "Studies in hydrodynamics and structure of stars and planets," *Astrophys. Norweg.* **4** (1946).
- Yoshimura, H., "Phase relation between the poloidal and toroidal solar-cycle general magnetic fields and location of the origin of the surface magnetic fields," *Solar Phys.* **50**, 3-23 (1976).

